OPEN

Citation: Cell Death and Disease (2014) 5, e1240; doi:10.1038/cddis.2014.203
© 2014 Macmillan Publishers Limited All rights reserved 2041-4889/14
www.nature.com/cddis

HKH40A downregulates GRP78/BiP expression in cancer cells

T Kosakowska-Cholody[1], J Lin[1,3], SM Srideshikan[1,3], L Scheffer[1], NI Tarasova[2] and JK Acharya*[,1]

HKH40A, the 8-methoxy analog of WMC79, is a synthetic agent with promising *in vitro* and *in vivo* antitumor activity, especially against solid tumors. However, molecular mechanisms underlying its antitumor effects are poorly understood. Here, we report that HKH40A markedly reduces the level of GRP78/BiP protein in cancer cell lines of various origin. In this study, we show that HKH40A not only downregulates transcription of GRP78 but also directly binds to the isolated protein and induces its proteosomal degradation. Knockdown of BiP increased the efficacy of the drug and overexpression of BiP diminished its activity. BiP is generally highly elevated in solid tumors having a pivotal role in cancer cell survival and chemoresistance, and has been suggested as a novel target for therapeutic intervention. We show that reduction of BiP level by HKH40A impairs its function and induces unfolded protein response as evidenced by the activation of IRE1α, ATF6 and PERK. This leads to a series of downstream events, including sustained eIF2α phosphorylation, increased abundance of spliced XBP1 mRNA and protein levels of ATF4 and CHOP. We also demonstrate that HKH40A inhibited tumor formation in an *in vivo* xenograft tumor model. Collectively, our data show that HKH40A reduces BiP levels and this could have an important role in the activity of HKH40A against cancer cells.

Cell Death and Disease (2014) **5,** e1240; doi:10.1038/cddis.2014.203; published online 22 May 2014
Subject Category: Cancer Metabolism

Reprogramming of energy metabolism and increasing dependence on glycolysis is one of the principal hallmarks of cancer.[1] Glucose deprivation in cancer cells leads to the accumulation of under-glycosylated and misfolded proteins in the lumen of the endoplasmic reticulum (ER stress), and triggers the unfolded protein response (UPR).[2,3] Also, the rapidly proliferating cancer cells require increased ER activity to accommodate high demands for protein folding and assembly. All these lead to an increase in baseline ER stress in tumor cells as compared with normal cells.

The primary sensor and master regulator of the ER stress is glucose-regulated protein 78 (GRP78, also known as BiP). As an ER chaperone, BiP is involved in numerous functions, including translocation of nascent polypeptides, facilitation of *de novo* protein folding and assembly, targeting of misfolded proteins to ERAD and maintenance of calcium homeostasis. GRP78/BiP has critical cytoprotective roles in oncogenesis and its increased expression has been observed in many cancers.[4–9] BiP overexpression confers resistance to a variety of chemotherapeutic agents, and knockdown of BiP sensitizes tumor cells to drug treatment.[10–13] Treatment with many anticancer agents further induces BiP and results in enhanced drug resistance.[11,14–16] BiP-mediated resistance is not limited to proliferating tumor cells. Knockdown of BiP also induces strong killing of dormant cancer cells treated with doxorubicin,[17] suggesting that drugs targeting BiP could help to eradicate residual tumor. Given the importance of BiP in cancer cell survival, progression and chemoresistance, it represents a prime target for anticancer agents.[3,18–23] Currently, NKP-1339 (IT-139) is the only drug in clinical trials that is claimed to interfere with the BiP pathway.[24] Discovery of other agents that target this pathway would be of great value.

The bisimidazoacridones and related compounds discovered and developed at the NCI constitute a new class of highly potent, multifunctional anticancer agents with a significant selectivity against solid tumors.[25–30] They accumulate in the nuclei of treated cells and bind to DNA and dysregulate expression of many important genes.[28] However, the exact mechanism of action at molecular level is not fully understood. WMC-79, the best known compound in this series, was found to be a selective cytotoxic agent in a number of tumor cell lines.[26,28] Optimization of WMC-79 led to HKH40A, which was selected for preclinical development as the most active compound in this class.[26,27,29] HKH40A is unique as it simultaneously targets several hallmark capabilities of cancer. HKH40A blocks uncontrolled replication of cancer cells by reducing Cdc6, Cdc7 and ribonucleotide reductase M2 (RRM2) levels. It counteracts evading growth suppressors by activating p53 and pRB.[29] The compound overcomes another important hallmark of cancer, the resistance to cell death, by triggering apoptosis.[29,31] Herein, we describe the

[1]Laboratory of Cell and Developmental Signaling, National Cancer Institute at Frederick, Frederick, MD, USA and [2]Cancer and Inflammation Program, National Cancer Institute at Frederick, Frederick, MD, USA
*Corresponding author: JK Acharya, Laboratory of Cell and Developmental Signaling, National Cancer Institute at Frederick, Rm 22-90B, Bldg 560, 1050 Boyles Street, Frederick, MD 21702, USA. Tel: +1 301 846 7051; Fax: +1 310 846 1666; E-mail: acharyaj@mail.nih.gov
[3]These authors contributed equally to this work.
Keywords: HKH40A; GRP78/BiP; unfolded Protein Response (UPR); chemoresistance; cancer; paraptosis
Abbreviation: GRP78/BiP, glucose-regulated protein 78/BiP; ER, the endoplasmic reticulum; UPR, unfolded protein response; TG, thapsigargin; h, hours
Received 06.1.14; revised 08.4.14; accepted 09.4.14; Edited by H-U Simon

discovery of downregulation of GRP78/BiP in cancer cells treated with HKH40A and demonstrate that this effect is not only due to the inhibition of transcription but also direct interaction of the compound with BiP causing enhanced proteasomal degradation. We show that reduction of BiP levels triggers a sustained activation of the UPR leading to the apoptotic and non-apoptotic cancer cell death. Knockdown and overexpression of BiP affected the efficacy of HKH40A indicating that downregulation of BiP is one of the contributing factors in its antitumor effect.

Results

HKH40A activates the UPR by downregulating GRP78/BiP. BiP levels are upregulated in many cancers including several cancer cell lines and this is believed to protect cells against stress-induced apoptosis. Since HKH40A (Figure 1a) is a potent antitumor agent, we evaluated whether part of its action was due to disruption of BiP-mediated protective mechanisms. We treated HCT-116 and HT-29 colon cancer cell lines with 100 nM HKH40A for 6, 24 and 48 h. Western blot analysis showed reduction of BiP expression in both cell lines after 6 h treatment and was more pronounced at later time points (Figure 1b).

In non-stressed cells, BiP binds and inhibits IRE1α (inositol-requiring protein 1 alpha), ATF6 (activating transcription factor 6) and PERK (PKR-like ER kinase), the three sentinels of the UPR pathway. Upon induction of ER stress, BiP is recruited by the misfolded proteins and is consequently disengaged from the three sentinels.[32] After release from BiP, the three sensors undergo autoactivation and induce UPR signaling cascade. Activated IRE1α removes 26-nucleotide intron from the mRNA encoding X-box binding protein 1 (XBP1). The spliced XBP1 activates expression of a group of ER chaperones and enzymes to help protein folding, maturation, secretion, as well as degradation of misfolded proteins. After dissociation from BiP, ATF6 translocates to the Golgi where it is proteolytically cleaved and subsequently activates the expression of UPR targets genes.

Activated PERK phosphorylates translation initiation factor eI2Fα, leading to protein translational attenuation in general, which reduces the ER workload and provides a survival signal. However, PERK-mediated eI2Fα phosphorylation also leads to preferential translation of specific mRNAs, one of which encodes the activating transcription factor 4 (ATF4). ATF4 subsequently activates the pro-apoptotic factor GADD153/CHOP to mediate ER stress-associated apoptosis. Therefore, we evaluated whether HKH40A-induced reduction of BiP causes changes in expression of the three sentinels and thereby affect the signaling pathways of the UPR.

HKH40A treatment not only resulted in phosphorylation of IRE1α on Ser724 but also increased total levels of the protein (Figure 1b). Activation of IRE1α was also confirmed by the appearance of the spliced form of *XBP1* (Figure 1c). In cells treated with HKH40A, ATF6 was activated, converting the full length (p90 ATF6) to its activated 50-kDa form (p50 ATF6) (Figure 1b). Significant phosphorylation of PERK on Thr981 was evident as early as 6 h and was accompanied by sustained phosphorylation of eIF2α. Activation of PERK cascade was additionally supported by increased expression of ATF4 and CHOP in both cancer cell lines. We also observed translocation of these proteins to the nucleus in HCT-116 cells (Supplementary Figure S1). Collectively, these data indicate that HKK40A activates UPR by downregulating BiP in these cells. Other members of the Hsp70 family, GRP75 and HSP70, as well as other ER chaperone proteins like PDI and GRP94 were not affected by HKH40A treatment (Figure 1d).

Downregulation of BiP levels was additionally confirmed by confocal microscopy of HCT-116 and HT-29 cells immunostained with the BiP antibody (Figure 2a). Both cell lines displayed a high basal level of BiP that was markedly reduced by HKH40A treatment, especially after 48 h. Cells exposed to 150 nM of TG for 24 h was used as a positive control.

HKH40A reduces BiP in various types of cancer cells. We next evaluated whether HKH40A downregulates BiP in other cancer cells. Western blot analysis showed that treatment with HKH40A significantly reduced the basal level of BiP also in liver (HepG2 and Hep3B), pancreatic (Panc10.05 and AsPC-1) and glioma (SF268) cancer cell lines (Figure 2b). Hence, downregulation of BiP by HKH40A is not only specific to colorectal but also to other cancer cells.

BiP downregulation is critical for HKH40A cytotoxicity. We asked whether BiP overexpression or knockdown modulated HKH40A activity in these cell lines. First, we created a stable cell line that genetically overexpresses BiP. We analyzed the levels of BiP after drug treatment in HCT-116 and BiP-overexpressing HCT-116 CMV-BiP cells. In both cells, HKH40A reduced BiP in a time-dependent manner; however, the levels were even higher in HCT-116 CMV-BiP cells (Figure 3a). Next, using MTT assay we determined activity of the drug in both cell lines. We found that cells with overexpressed BiP are more resistant to the drug but only at early time points (Figure 3c). At later time points, when BiP levels were downregulated, even cells that overexpressed BiP succumbed to the effect of HKH40A. We also determined whether downregulation of BiP could influence activity of HKH40A. We used siRNA to knockdown the levels of BiP (Figure 3b) and evaluated activity of the drug by using an MTT assay (Figure 3c). Cells that were transfected with BiP siRNA were more sensitive to the drug treatment compared with control cells. The most prominent difference, about 40%, was detected after 48 h treatment (Figure 3c). We also observed that transfection with BiP siRNA alone without drug treatment did not affect the cell growth as compared with control siRNA.

Therefore, BiP overexpression and knockdown experiments indicate that the abiltiy of the drug to downregulate BiP enhances the sensitivity of these cells to the other cytotoxic effects of HKH40A.

HKH40A downregulates GRP78/BiP transcription. We then sought to determine the mechanisms underlying the downregulation of BiP by HKH40A treatment. Data from qPCR analysis showed that treatment with 100 nM HKH40A for 24 h, in both HCT-116 and HT-29 cells, decreased the BiP mRNA level to about 43 and 67%, respectively (Figure 4a). To probe whether the downregulation of BiP mRNA level was

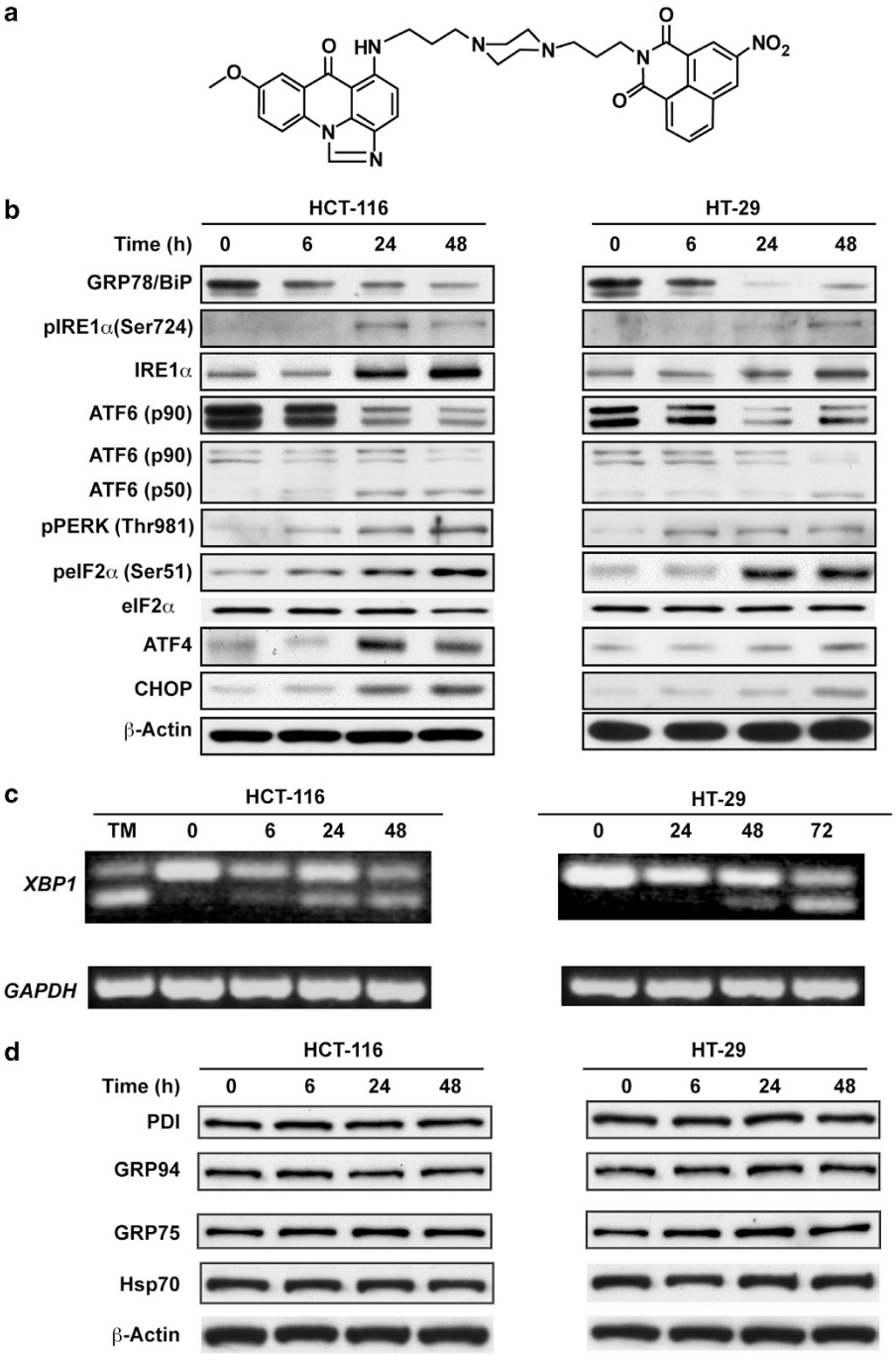

Figure 1 Selective downregulation of BiP and activation of the UPR signaling pathways by HKH40A. (**a**) Chemical structure of HKH40A; (**b**) Representative protein bands from western blot analysis. HCT-116 and HT-29 cells were cultured for the indicated time in the presence of 100 nM HKH40A. Total cell lysates were subjected to western blot analysis with specific antibodies as indicated, β-actin was used as a loading control. ATF6 was probed with two different antibodies. The top panel was probed by a rabbit polyclonal that only detects total ATF6 (p90). The bottom panel was probed by the mouse monoclonal antibody from Abcam that detects both full-length ATF6 (p90) and cleaved products ATF6 (p50). (**c**) Analysis of XBP1 splicing by RT-PCR using XBP1-specific primers. Tunicamycin (TM) (2.5 μM) treatment was used as positive control and GAPDH was internal control. (**d**) Western blot analysis of other ER chaperons in HCT-116 and HT-29 cells treated with 100 nM HKH40A

due to transcriptional inhibition, we performed reporter assays using a 1057-bp BiP promoter fragment. The reporter activities in transfected cells with pGL3-Bip-1057 were decreased about 54 and 62% in HCT-116 and HT-29 cells, respectively (Figure 4b). These data suggest that HKH40A could partially inhibit BiP's transcription.

HKH40A directly binds to BiP and could induce its degradation. BiP has been reported to have half-life that is generally greater than 24 h.[33,34] Since we noted downregulation of BiP in less than 24 h, transcriptional downregulation might not explain the decreased BiP levels noted in short-term experiments. Therefore, we asked

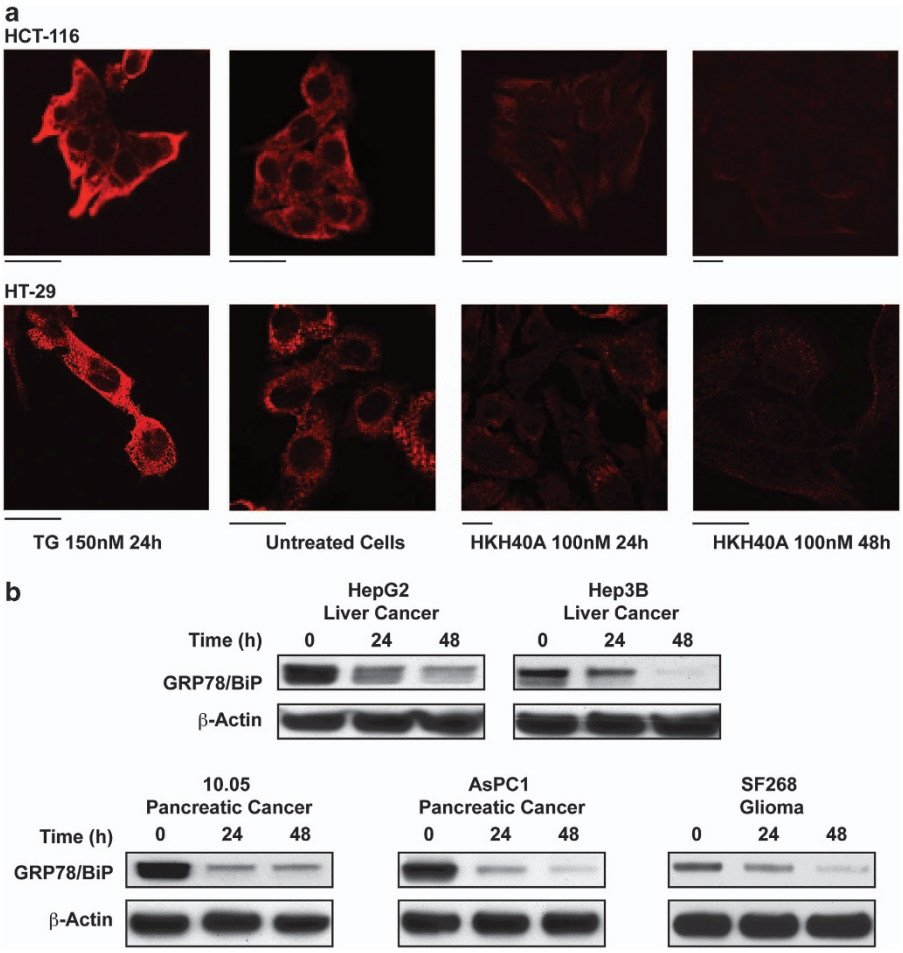

Figure 2 Downregulation of BiP by HKH40A in different cell lines. (**a**) Representative confocal microscopy images of HCT-116 and HT-29 cells untreated and treated with HKH40A. Cells were immunostained for BiP (red). Thapsigargin (TG) was used as a positive control. Scale bar = 20 μm. (**b**) Western blot analysis of BiP expression in selected cancer cell lines treated for indicated times with 100 nM HKH40A

whether other mechanisms could explain the effects of HKH40A on BiP levels.

We took advantage of the intrinsic fluorescence of HKH40A that allowed its visualization by confocal microscopy. HKH40A, upon excitation at 488 nm, emits green fluorescence.[35] HCT-116 cells were treated with HKH40A, fixed and immunostained for BiP. As shown in Figure 5a, the drug mostly accumulated in the nucleus where it bound to DNA and emitted very bright fluorescence. The intrinsic fluorescence of HKH40A increases 40-fold upon binding DNA.[35] Weaker green fluorescence was visible in the cytoplasm. Immunostaining of cells with the BiP antibody showed perinuclear and cytoplasmic localization. We also noticed some overlap of the two signals in the perinuclear region indicating that HKH40A could colocalize with BiP in the ER, suggesting a possibile direct drug–protein interaction. To assess whether HKH40A is capable of binding BiP, we applied microscale thermophoresis (MSN) using the titration of the compound with recombinant human BiP. The method is based on the ligand binding-induced changes in the movement of fluorescent molecules along a temperature gradient.[36–38] We used intrinsic fluorescence of HKH40A for the measurements. Addition of GRP78/BiP caused significant and concentration-dependent changes in thermophoretic mobility of HKH40A that are indicative of direct binding (Figure 5b). The determined apparent K_D of interaction was 788 ± 107 nM assuming that all molecules in the commercial preparation of BiP have been folded correctly and active.

We then asked whether BiP was being subject to degradation upon binding to HKH40A. Proteasomal degradation is the main pathway for cellular degradation of proteins. In order to address involvement of this pathway, we used the proteasome inhibitor MG132. As shown in Figure 5c, protein level was significantly reduced in cells treated with HKH40A alone. However, in cells exposed to the combined treatment or MG132 alone, we detected slightly increased level of BiP. These data suggest that MG132 rescued the BiP protein from degradation induced by HKH40A treatment.

Thus, HKH40A could target BiP for proteasomal degradation. This could be responsible for the rapid decline in BiP levels observed in cancer cells upon treatment with the drug. In addition, transcriptional downregulation by inhibition of the promoter could reduce the transcript levels over time in these treated cells.

Topoisomerase1 and 2 inhibition is not implicated in the reduction of BiP level by HKH40A. Symmetrical bisimidazoacridones like WMC-26 and the unsymmetrical compounds like WMC-79 and HKH40A bind strongly to DNA.[35] Only unsymmetrical imidazoacridones are potent catalytic inhibitors of topoisomerase1 and 2 (Supplementary Figure S2).

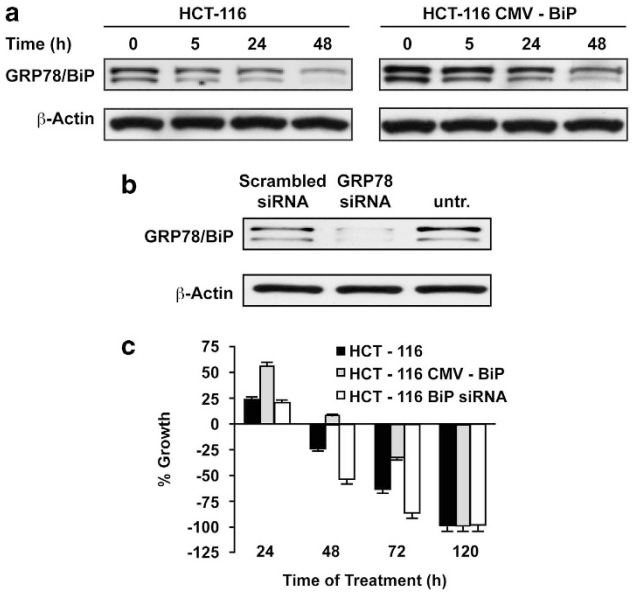

Figure 3 Stable gene overexpression and knockdown of BiP by siRNA and the effect of HKH40A in these cells. (**a**) Western blot analysis of BiP in HCT-116 and cells with overexpressed BiP (HCT-116 CMV-BiP) after treatment with 100 nM HKH40A. (**b**) siRNA knockdown of BiP in HCT-116 cells 48 h after transfection examined by western blot. (**c**) Effect of HKH40A in cells with overexpressed (HCT-116 CMV-BiP) or reduced BiP (HCT-116 BiP siRNA). HCT-116 control, transfected with siRNA and cells with overexpressed BiP were seeded in 96-well plates. Forty-eight hours after plating, the cells were treated with 100 nM HKH40A and cytotoxicity was determined by using an MTT assay

To explore whether inhibition of topoisomerase1 and 2 is implicated in HKH40A-mediated reduction of BiP, we tested side-by-side HKH40A, WMC26, camptothecin (topoisomerase1 inhibitor), and etoposide and doxorubicin (topoisomerase2 inhibitor). In HT-29 cells, only HKH40A and WMC26 were able to reduce the level of BiP expression, whereas camptothecin, etoposide and doxorubicin could not (Figure 5d). These results suggest that topoisomerase1 or topoisomerase2 inhibitory properties of HKH40A are not involved in the reduction of BiP levels.

HKH40A inhibits tumor formation in a model of colon cancer xenografts in nude mice. Previous xenograft studies demonstrated that BiP is required for tumor initiation and progression.[39] To test the effects of HKH40A on the progression of tumors produced by subcutaneous implantation of HCT-116 cancer cells, we pretreated the cells for 24 h with 100 nM HKH40A (when the BiP level was very low and cell viability was more than 90%) in athymic nude mice. Mice were injected bilaterally (right side-vehicle treated cells; left side-HKH40A treated cells). Twenty-eight days after injection, we did not observe any tumor formation on the left side of any animals where cells treated with HKH40A were injected. Whereas, on the right side inoculated with vehicle-treated cells (5% glucose), tumors with median volume about 1000 mm^3 were present in all animals (Figures 6a–c). Thus, we demonstrate that HKH40A-treated cancer cells fail to grow in a xenograft model of mouse.

HKH40A induces paraptosis in parallel to apoptosis. Previously it was reported that HKH40A treatment of cancer cells triggers cell death mediated mainly by apoptosis.[29,31] Cell cycle analysis by FACS and annexin staining studies were done to analyze cell death. We noticed cell death in both cell lines but significantly more in HCT-116 compared with HT-29 (Supplementary Figures S3a and b). Recent report connecting phosphorylation of eIF2α and the UPR with

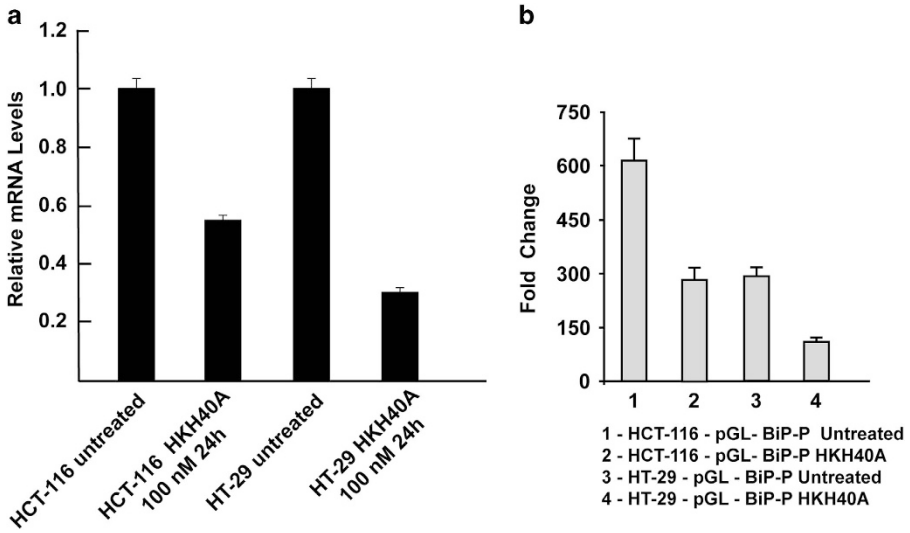

Figure 4 HKH40A affects transcription of GRP78/BiP. (**a**) qPCR analysis of BiP transcripts in HCT-116 and HT-29 cells untreated or treated with 100 nM HKH40A for 24 h. (**b**) Promoter activity in HCT-116 and HT-29 cells transfected with pGL-BiP-P plasmid and treated with 100 nM HKH40A for 24 h (fold change relative to pGL-4.10 empty vector transfected cells)

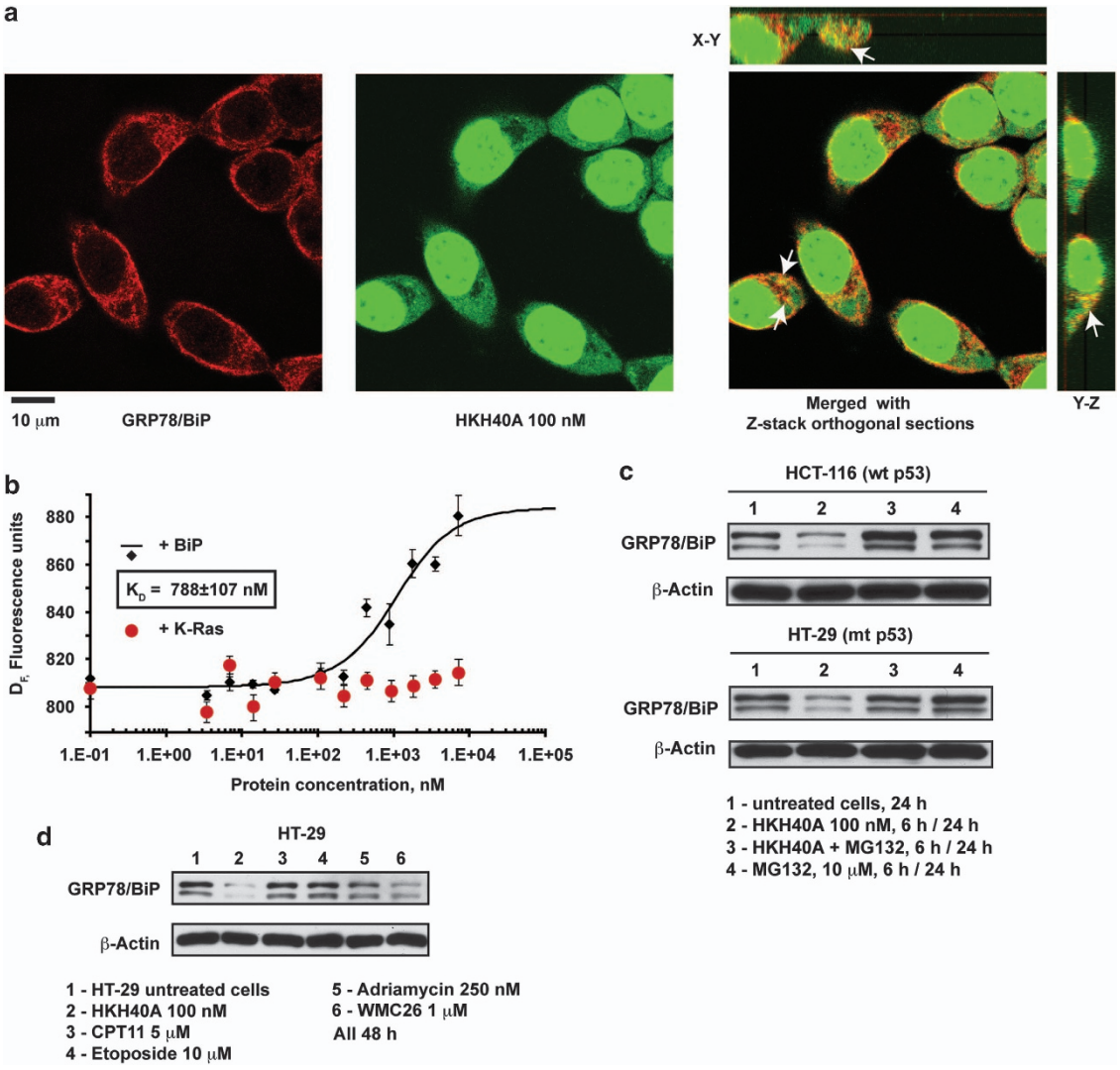

Figure 5 HKH40A directly binds BiP and affects its stability. (**a**) Colocalization of HKH40A with BiP. HCT-116 cells were treated with 100 nM HKH40A for 3 h, fixed and immunostained for GRP78. The drug with intrinistic ability to fluoresce binds to DNA and emits very bright fluorescence. Fluorescence is also visible in cytoplasm. Immunostaining of cells with GRP78 shows perinuclear and cytoplasmic localization. Some overlap of the two signals in the perinuclear region can be noted in the orthogonal views of the Z-stacks, scale bar 10 μm. (**b**) Direct interaction of HKH40A with recombinant human GRP78/BiP. Microscale thermophoresis analysis revealed direct interaction of HKH40A with recombinant human GRP78/BiP. Analysis was performed using the intrinsic ability of HKH40A to fluoresce. Purified recombinant human K-Ras (1–166) was used as a negative control (in red). Its addition caused no change in the thermophoretic mobility of the compound. (**c**) Proteosomal degradation is involved in HKH40A downregulation of BiP. HCT-116 and HT-29 cells were treated with 100 nM HKH40A, 10 μM MG132 or a combination of both agents for 6 h, then drugs were removed, cells were cultured in a drug-free medium for up to 24 h, collected and analyzed by western blot. (**d**) Topoisomerase1 and topoisomerase2 inhibition is not responsible for the reduction of GRP78/BiP level by HKH40A. HT-29 cells were cultured for 24 h with vehicle (1), 100 nM HKH40A (2), 5 μM CPT-11 (3), 10 μM Etoposide (4), 250 nM adriamycin (5) and 1 μM WMC26 (6). Total cell lysates were subjected to western blots with anti-GRP78/BiP. β-Actin was used as a loading control

paraptosis,[40] prompted us to investigate whether HKH40A triggers this type of caspase-independent cell death.

Paraptosis is characterized by extensive cytoplasmic vacuolization that begins with progressive swelling of mitochondria and the endoplasmic reticulum (ER). Light microscopy images of HCT-116 and HT-29 cells treated with HKH40A showed marked changes in cellular morphology. In addition to floating apoptotic cells, we noticed presence of cells with massive cytoplasmic vacuolization (Supplementary Figure S4a), a feature of paraptosis, indicating that HKH40A could also trigger this type of death.[41,42]

In addition to vacuolization, we observed progressive swelling of the mitochondria that is consistent with paraptosis (Supplementary Figure S4b). Kinetically, paraptosis is slower than apoptosis and requires MAP kinase activation.[43] We observed a time-dependent upregulation of phosphorylated ERK and JNK kinases and sustained activation of the MAPK pathway in HKH40A-treated cells (Supplementary Figure S4c).

However, plasma vacuolization is a characteristic of not only paraptosis but also of autophagy, and mitochondrial swelling can be detected in apoptotic, paraptotic and necrotic cell death. In order to evaluate what type of cell death is predominant after HKH40A treatment, HCT-116 and HT-29 cells were treated with HKH40A along with the caspase inhibitor Z-VAD-FMK, UO126 (MAPK's inhibitor), 3-MA

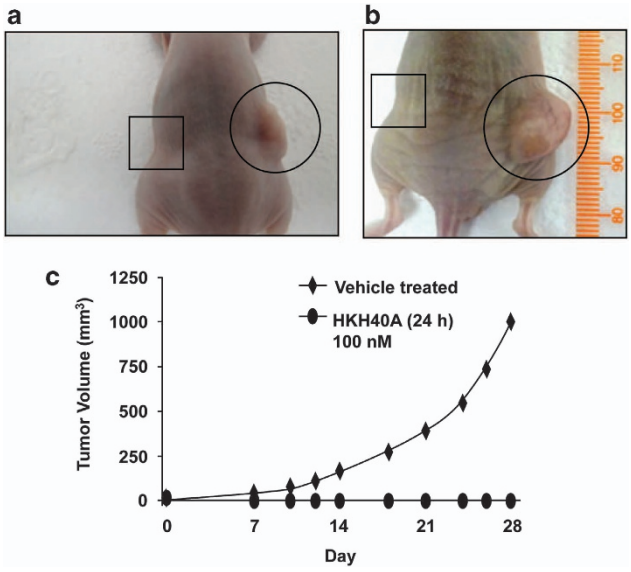

Figure 6 HKH40A inhibits tumor formation in mouse xenograft model. Representative photographs of mice were taken at day 12 (**a**) and day 28 (**b**) after inoculation of 1×10^7 HCT-116 treated with vehicle (right side-circle) and treated with100 nM HKH40A for 24 h (left side-square). (**c**) Growth curves of the treated and untreated xenograft tumors

(an autophagy inhibitor) and Nec-1 (necroptosis inhibitor). Z-VAD-FMK almost totally inhibited drug-induced cell death in HCT-116 cells at 48 h (Supplementary Figure 4d). However, longer exposure to the drug gradually reduced the death inhibiting potential of Z-VAD-FMK to 50 and 10% after 72 and 120 h treatment, respectively, which suggests that the HKH40A is able to overcome inhibition of apoptosis by inducing caspase-independent cell death. In contrast, Z-VAD-FMK only partially inhibited cell death in HT-29 cells, indicating that in this cell line the drug-induced death is also caspase independent (Supplementary Figure S4d).

To determine the involvement of MAPK pathway, UO126, a specific inhibitor of MEK1 and 2, was used. UO126 had only negligible effect on activity of HKH40A in HCT-116 (Supplementary Figure 4d). However, the MAPK pathway appears to be more involved in the death process in HT-29 cells where the inhibitor significantly reduced cytotoxicity of HKH40A. But, Nec-1 and 3-MA showed no effect on cell death or vacuolization of HKH40A-treated cells, ruling out autophagy and necroptosis (Supplementary Figure S4d).

It is worth noting here that the mitochondrial swelling observed in these cells were associated with decreased mitochondrial membrane potential as observed by FACS analysis (Supplementary Figure S5). Staining cells with MitoSox Red followed by FACS analysis showed (Supplementary Figure S6) that generation of reactive oxygen species (ROS) was not an initiation factor for cell death as attached cells did not show ROS production while only a fraction of the floating cells were ROS positive.

Discussion

BiP is highly elevated in solid tumors and many cancer cell lines.[3] It is not only present in the ER but is also found in the cytoplasm, nucleus and plasma membrane. The wide range of cellular functions and localization of BiP contribute to novel signaling functions and processes that regulate proliferation, apoptosis and immunity. The diverse functions of BiP also have an important role in the acquisition of cancer hallmarks by tumor cells making it an ideal drug target for effective cancer treatment.[44]

We have presented evidence that HKH40A strongly downregulates BiP levels in several cancer cell lines (eg, the colon, liver, pancreas, brain). Our study also showed that decrease in the levels of BiP in cancer cells after HKH40A treatment impairs its function to sequester IRE1α, ATF6 and PERK and activates all three UPR transducers pathways resulting in increased expression of UPR target genes including ATF4 and CHOP/GADD153. Excessive eI2Fα phosphorylation leading to induction of the pro-apoptotic GADD153 is poorly tolerated and triggers apoptotic program as was demonstrated for pancreatic β-cells.[45] Sustained phosphorylation of eI2Fα suggests that HKH40A-mediated cell death could be partly due to activation of the PERK pathway leading to apoptosis. In addition to being a chaperone and regulator of UPR, BiP also regulates intracellular calcium levels. BiP maintains the ER calcium levels by preventing its efflux into cytosol, and conditions that downregulate BiP levels were associated with decreased ER calcium.[46,47] We have also observed decreased calcium levels in HKH40A-treated cells upon thapsigargin treatment (Supplementary Figures S7a and b).

We found that the reduction of BiP protein levels is a result of not only decreased transcription of its gene but also direct drug–protein binding and proteasomal degradation. Reduced transcription can be explained by the binding of HKH40A to BiP promoter as shown by our reporter assay. However, at this point we have no simple explanation for the enhanced degradation. On the basis of the fact that HKH40A binds to BiP, we can speculate that such direct interactions with the drug may cause a conformational change in the protein making it a better proteasomal substrate. Recently, it was reported that small molecules could bind to the ATPase domain of GRP78/BiP and facilitate dissociation of BiP complexes with other proteins.[48] Structurally, HKH40A can be considered a nucleotide mimetic. Thus, it is possible that HKH40A binds to the ATP site of BiP causing dissociation of the three ER stress sensors, and that the released monomeric 'naked' BiP is especially susceptible to degradation. However, to verify this hypothesis, further studies are required. Also, while overwhelming experimental evidence suggests a direct effect of HKH40A on BiP, we cannot entirely rule out other effects of HKH40A that might also lead to a reduction in BiP levels. The ability of HKH40A to downregulate BiP could also affect the function of normal cells and adversely affect cells that are dependent on BiP. However, previous *in vitro* experiments using noncancer cell lines, *in vivo* analysis of the drug in orthotopic model of liver cancer in rat and xenograft studies of human colon and pancreatic cancer indicate that HKH40A is less toxic to normal cells and tissues in the concentration range where it inhibits the growth of cancer cells.[29,31]

Together, the above findings suggest that induction of UPR by reduction of BiP expression could be an important additional mechanism of the anticancer activity of the multifunctional antitumor agent HKH40A. This finding provides a foundation for the rational design of combination therapies.

We believe that HKH40A can be particularly effective when combined with established anticancer drugs known to upregulate BiP that usually run into problems of chemoresistance (eg, gemcitabine (Gemzar) or Velcade). Previously, HKH40A was shown to produce a strong synergistic anticancer effect in combination with gemcitabine in mice xenografted with human pancreatic cancer MiaPaCa-2.[27] The rationale for this combination was based on the fact that HKH40A downregulates RRM2, the molecular target of gemcitabine, overexpression of which is responsible for gemcitabine resistance. Reduction of BiP/GRP78 levels in HKH40A and gemcitabine-treated cells (Supplementary Figure S7c) provides additional logical factor for the synergistic action.

We have also examined the form of cell death caused by HKH40A and have uncovered the involvement of other non-apoptotic form of death, paraptosis. Collectively, our study revealed that HKH40A triggers programmed cell death (PCD) not via a single specific pathway but rather via multiple pathways that may overlap with each other. Caspase-independent pathways mediated by HKH40A vary on the type of tumor cells and the applied death stimulus. In HKH40A-treated cells, we showed the occurence of paraptosis in parallel to apoptosis, as a consequence of reduced expression of GRP78/BiP followed by induction of UPR.[40]

In summary, HKH40A targets multiple principal hallmarks of cancer, making it a perfect candidate for further preclinical and clinical testing. It also possesses a great potential to enhance drug efficacy of a wide variety of conventional agents.

Materials and Methods

Chemicals. Cell culture media and reagents were obtained from Life Technologies (Grand Island, NY, USA). CPT-11, doxorubicin, etoposide and thapsigargin were from Sigma-Aldrich (St.Louis, MO, USA). 3- methyladenine (3-MA) was from MP Biomedicals, LLC (Solon, OH, USA), MG132, necrostatin-1 (NEC-1) were from EMD Biosciences (San Diego, CA, USA), U0126 was from Promega Corporation (Madison, WI, USA).

Cell lines and cell culture. The tumor cell lines HCT-116, HT-29, Hep3B, HepG2, AsPC-1, Capan2, MiaPaCa2, Panc10.05 and SF-268 were purchased from the ATCC (Rockville, MD, USA). HCT-116, HT-29, Hep3B, HepG2, Capan2 and MiaPaCa2 were cultured in Dulbecco's modified Eagle's medium, SF-268, AsPC-1 and Panc10.05 in RPMI 1640. For AsPC-1 and Panc10.05, medium was additionally supplemented with 10 mM MEM non-essential amino acids, 100 mM sodium pyruvate, 10 mM HEPES buffer and 0.2 unit/ml insulin. All cell lines were authenticated by the suppliers and were used within 6 months of receipt or resuscitation. The cells were not authenticated further by the authors.

Drug preparation procedure. HKH40A (NSC D 725785) was synthesized in NCI laboratory by the methods previously described.[27] HKH40A stock solution (5 mM) was prepared by dissolving its methanesulfonate salt form in water and stored at 4 °C. Before use, stock solution was diluted to a final concentration of 500 μM in distilled water and then used to prepare working solution in appropriate tissue culture media.

Western blotting. Immunoblot analysis of cell protein lysates was performed according to Santa Cruz Biotechnology, manufacturer's instructions as described previously.[28]

Antibodies. All primary antibodies used in this study are listed in Table 1. Secondary antibodies were from Jackson Immunoresearch (West Grove, PA, USA).

Confocal laser scanning microscopy for GRP78. A total of 5×10^4 HCT-116 or HT-29 cells were plated into 35 mm glass bottom dishes (MatTek Corporation, Ashland, MA, USA). Next day cells were treated with vehicle, 100 nM HKH40A or 150 nM of thapsigargin. After desired time of treatment, tissue cultures were rinsed with PBS, fixed for 20 min with 4% Paraformaldehyde (PFD), rinsed with PBS, permeabilized 3 min with 0.1% Triton-X, rinsed with PBS-0.05% Tween (PBS-T). After 1 h blocking of nonspecific binding sites using 5% bovine serum albumin (BSA), cells were stained 1 h with the primary antibody to GRP78/BiP (Rabbit polyclonal, ab21685, Abcam) diluted 1 : 500 in 5% BSA then washed with PBS-T, stained with secondary antibody Alexa 594 (1 : 1000 in 5% BSA) for 1 h followed by final PBS-T washes and examined using a Zeiss LC510 confocal microscope. All steps were performed at room temperature.

XBP1 splicing. The splice variant of XBP1 was evaluated using the primers and conditions as described in the Supplementary Data.

Inhibition of BiP expression by transient siRNA transfection. Three predesigned BiP-specific siRNA duplexes (SR302256A- 5′-rGrCrCrCrArArUrArCrArGrCrCrArUrUrArArArGrArUrGAC-3′; SR302256B—5′-rCrCrArUrArArGrUrGrArCrArCrCrArArUrArArArArUrGrUTT-3′; SR302256C—5′-rGrGrUrArUrGrArUrCrArArUrArArArGrGrArCrArGrGrCTG-3′) to knockdown BiP and universal scrambled negative control siRNA duplex (Trilencer-27 siRNA cat. # SR302256, OriGen Technologies, Rockville, MD, USA) were used in this study.

Introduction of siRNA duplexes into cancer cells was performed using electroporation with Amaxa Cell Line Nucleofector Kit V for HCT-116 cells (Lonza,

Table 1 Table of antibodies

Antibody	Company	Catalog number	Source and clonality	Dilution
β-Actin	Abcam, Cambridge, MA, USA	ab6276	Mouse, monoclonal	1 : 10 000
ATF4	Proteintech Group, Inc, Chicago, IL, USA	10835-1-AP	Rabbit, polyclonal	1 : 500
ATF-6 (total and cleaved)	Abcam	ab122897	Mouse, monoclonal	1 : 500
ATF-6 (total)	AnaSpec, San Jose, CA, USA	54252	Rabbit, polyclonal	1 : 1000
BiP (western blot)	Cell Signaling, Danvers, MA, USA	3177	Rabbit, monoclonal	1 : 1000
BiP (IF)	Abcam	ab21685	Rabbit, polyclonal	1 : 500
CHOP	Pierce, Rockford, IL, USA	MA1-250	Mouse, monoclonal	1 : 100
CHOP	Santa Cruz Biotechnology, Dallas, TX, USA	sc-575	Rabbit, polyclonal	1 : 100
eIF2α	Cell Signaling	9722	Rabbit, polyclonal	1 : 1000
p-eIF2α(Ser51)	Abcam	ab32157	Rabbit, monoclonal	1 : 1000
GRP75	Cell Signaling	2816	Rabbit, polyclonal	1 : 1000
GRP94	Cell Signaling	2104	Rabbit, polyclonal	1 : 2000
Histone H3	Abcam	ab8895	Rabbit, polyclonal	1 : 1000
HSP70	Cell Signaling	4872	Rabbit, polyclonal	1 : 2000
IRE1α	Cell Signaling	3294	Rabbit, monoclonal	1 : 1000
p-IRE1α(Ser724)	Novus Biological, Littleton, CO, USA	NB100-2323	Rabbit, polyclonal	1 : 1000
p-PERK(Thr981)	Santa Cruz Biotechnology	Sc-32577	Rabbit, polyclonal	1 : 100
PDI	Cell Signaling, Abcam	3501	Rabbit, monoclonal	1 : 2000

Germany). Once the transfection was complete, the samples in the pre-equilibrated culture medium were gently transferred into 6-well or 96-well plates and incubated under growth conditions. Forty-eight hours post transfection, cells from 96-well plates were used for an MTT assay to evaluate cytotoxicity of HKH40A at different time points, and cells from six-well plate were collected and used for western blot to detect the level of BiP at the time of drug treatment.[28] Experiments were performed twice with similar results.

Establishment of the stable HCT-116 cell line overexpressing GRP78/BiP. Plasmid CMV-BiP was purchased from GeneCopoeia (Rockville, MD, USA) (Catalog # EX-T3592-M68). CMV-BiP was transfected into HCT-116 cells and selected by 2 μg/ml puromycin. Ten days later, the single colonies were picked and cultured. The BiP-overexpresing cell line was selected by checking its level using western blot.

MTT Assay. Control HCT-116, HCT-116 CMV-BiP (with overexpressed BiP) and HCT-116 cells transfected with BiP siRNA were seeded into 96-well microtiter plates (100 μl of medium containing 1500 cells per well). After 48 h (when the lowest level of BiP was detected after transfection), 100 μl of drug containing medium or medium only (control) was added to each well. The cytotoxicity was determined by the MTT-based CellTiter96 Non-Radioactive Cell Proliferation Assay (Promega) according to the manufacturer's protocol with minor changes.[28] While the drugs were added, assays were performed on extra reference plates to determine the cell population density at time 0 (T_0). After desired time, the assays were performed on test (T) and control (C) cells. The absorbance of the wells was determined at 570 nm by a Versa-max microplate reader (Molecular Devices, Sunnyvale, CA, USA). Cellular responses were calculated using the formula: $100 \times [(T - T_0)/(C - T_0)]$ for $T > T_0$ and $100 \times [(T - T_0)/T_0]$ for $T < T_0$).

Quantitative real-time RT-PCR. First-strand cDNA was synthesized as described previously.[49] Real-time quantitative PCR was performed in the Applied Biosystems 7500 Fast Real-time PCR System (Invitrogen, Grand Island, NY, USA) using iTaq universal SYBR Green supermix (Bio-Rad, Hercules, CA, USA). Each sample was analyzed in triplicate with GAPDH as the internal control. The primer sequences for different genes are listed as follows:

GRP78/BiP-Forward: 5′-GGAAAGAAGGTTACCCATGC-3′
GRP78/BiP-Reverse: 5′-AGAAGAGACACATCGAAGGT-3′
GAPDH-Forward: 5′-ACCATCTTCCAGGAGCGAG-3′
GAPDH-Reverse: 5′-TAAGCAGTTGGTGGTGCAG-3′

Luciferase assay. A 1057-bp (-958 to $+99$) human BiP promoter fragment was amplified from Bac vector RP11-96J20 and cloned into pGL4.10. The plasmid named pGL-Bip-P was transfected into HCT-116 and HT-29 cells with a reporter plasmid carrying the firefly luciferase gene under the control of the BiP promoter and a reference plasmid pRL-CMV-Renilla carrying the Renilla luciferase gene using Lipofectamine 2000 transfection reagent (Invitrogen). Twenty-four hours after transfection, cells were treated with 100 nM HKH40A. Firefly and Renilla luciferase activities were measured using a Dual-Luciferase Reporter Assay System (Promega) and a luminometer (NovStar, Bmg Labtech GmbH, Offenburg, Germany), and relative luciferase activity was calculated. Values were averaged from triplicate determinations.

Microscale thermophoresis HKH40A–BiP interaction studies. Binding of HKH40A to BiP protein was characterized by microscale thermophoresis.[36–38] Titration series have been prepared that contained constant amount of the compound in 15 probes and varying concentrations of the recombinant human protein (StressMarq). HKH40A concentration was 600 nM. Lower concentrations could not be used because of limited detection sensitivity. Final buffer composition included 20 mM Tris/HCl pH 7.5, 0.175 mM NaCl, 5% glycerol and 0.25 mM DTT. The highest protein concentration used (7 μM) was defined by protein solubility. The measurements were taken in standard treated capillaries on Monolith NT.115 instrument (NanoTemper Technologies GmbH, Germany) using 60% IR-laser power and LED excitation source with $\lambda = 470$ nm. Dissociation constant was calculated by NanoTemper Analysis 1.5.41 software using the K_D fit method. Purified recombinant human K-Ras (1–166) was used for the negative control.

Mouse xenograft studies. In this experiment, we used five six-week-old female inbred athymic nude mice from Charles Rivers (Frederick, MD, USA). Tumors were produced by subcutaneous injection of 1×10^7 colon cancer HCT-116 cells, treated with vehicle (5% glucose) into the right side and treated with 100 nM HKH40A for 24 h into the left side of mice. Animals were observed daily and tumor size was measured every third day. Length and width was measured to calculate the tumor volume ($LW^2/2$). The Institutional Animal Care and Use Committee at NCI Frederick approved the experiment, animal handling and experimental procedure.

Conflict of Interest

The authors declare no conflict of interest.

Acknowledgements. This study is dedicated to the memory of Dr. Chris Michejda who pioneered the synthesis, development and study of Bisaminacridones as antitumor agents at the National Cancer Institute for two decades and without whose contributions this study would not have been possible. We thank Ms. Katie Nyswaner, Dr. Balamurugan Kuppusamy, Dr. Shyam Sharan, Dr. Ira Daar, Dr. Usha Acharya and Dr. W. Marek Cholody for critical comments and discussions.

1. Hanahan D, Weinberg RA. Hallmarks of cancer: the next generation. *Cell* 2011; **144**: 646–674.
2. Kaufman RJ. Stress signaling from the lumen of the endoplasmic reticulum: coordination of gene transcriptional and translational controls. *Genes Dev* 1999; **13**: 1211–1233.
3. Luo B, Lee AS. The critical roles of endoplasmic reticulum chaperones and unfolded protein response in tumorigenesis and anticancer therapies. *Oncogene* 2013; **32**: 805–818.
4. Uramoto H, Sugio K, Oyama T, Nakata S, Ono K, Yoshimastu T *et al.* Expression of endoplasmic reticulum molecular chaperone Grp78 in human lung cancer and its clinical significance. *Lung Cancer* 2005; **49**: 55–62.
5. Scriven P, Coulson S, Haines R, Balasubramanian S, Cross S, Wyld L. Activation and clinical significance of the unfolded protein response in breast cancer. *Br J Cancer* 2009; **101**: 1692–1698.
6. Xing X, Li Y, Liu H, Wang L, Sun L. Glucose regulated protein 78 (GRP78) is overexpressed in colorectal carcinoma and regulates colorectal carcinoma cell growth and apoptosis. *Acta Histochem* 2011; **113**: 777–782.
7. Daneshmand S, Quek ML, Lin E, Lee C, Cote RJ, Hawes D *et al.* Glucose-regulated protein GRP78 is up-regulated in prostate cancer and correlates with recurrence and survival. *Hum Pathol* 2007; **38**: 1547–1552.
8. Zheng HC, Takahashi H, Li XH, Hara T, Masuda S, Guan YF *et al.* Overexpression of GRP78 and GRP94 are markers for aggressive behavior and poor prognosis in gastric carcinomas. *Hum Pathol* 2008; **39**: 1042–1049.
9. Langer R, Feith M, Siewert JR, Wester HJ, Hoefler H. Expression and clinical significance of glucose regulated proteins GRP78 (BiP) and GRP94 (GP96) in human adenocarcinomas of the esophagus. *BMC Cancer* 2008; **8**: 70.
10. Pyrko P, Schonthal AH, Hofman FM, Chen TC, Lee AS. The unfolded protein response regulator GRP78/BiP as a novel target for increasing chemosensitivity in malignant gliomas. *Cancer Res* 2007; **67**: 9809–9816.
11. Baumeister P, Dong D, Fu Y, Lee AS. Transcriptional induction of GRP78/BiP by histone deacetylase inhibitors and resistance to histone deacetylase inhibitor-induced apoptosis. *Mol Cancer Ther* 2009; **8**: 1086–1094.
12. Roue G, Perez-Galan P, Mozos A, Lopez-Guerra M, Xargay-Torrent S, Rosich L *et al.* The Hsp90 inhibitor IPI-504 overcomes bortezomib resistance in mantle cell lymphoma in vitro and in vivo by down-regulation of the prosurvival ER chaperone BiP/Grp78. *Blood* 2011; **117**: 1270–1279.
13. Al-Rawashdeh FY, Scriven P, Cameron IC, Vergani PV, Wyld L. Unfolded protein response activation contributes to chemoresistance in hepatocellular carcinoma. *Eur J Gastroenterol Hepatol* 2010; **22**: 1099–1105.
14. Zhang L, Wang S, Wangtao, Wang Y, Wang J, Jiang L *et al.* Upregulation of GRP78 and GRP94 and its function in chemotherapy resistance to VP-16 in human lung cancer cell line SK-MES-1. *Cancer Invest* 2009; **27**: 453–458.
15. Kern J, Untergasser G, Zenzmaier C, Sarg B, Gastl G, Gunsilius E *et al.* GRP-78 secreted by tumor cells blocks the antiangiogenic activity of bortezomib. *Blood* 2009; **114**: 3960–3967.
16. Wang J, Yin Y, Hua H, Li M, Luo T, Xu L *et al.* Blockade of GRP78 sensitizes breast cancer cells to microtubules-interfering agents that induce the unfolded protein response. *J Cell Mol Med* 2009; **13**: 3888–3897.
17. Ranganathan AC, Zhang L, Adam AP, Aguirre-Ghiso JA. Functional coupling of p38-induced up-regulation of BiP and activation of RNA-dependent protein kinase-like endoplasmic reticulum kinase to drug resistance of dormant carcinoma cells. *Cancer Res* 2006; **66**: 1702–1711.
18. Park HR, Tomida A, Sato S, Tsukumo Y, Yun J, Yamori T *et al.* Effect on tumor cells of blocking survival response to glucose deprivation. *J Natl Cancer Inst* 2004; **96**: 1300–1310.
19. Boelens J, Lust S, Offner F, Bracke ME, Vanhoecke BW. Review. The endoplasmic reticulum: a target for new anticancer drugs. *In Vivo* 2007; **21**: 215–226.

20. Lee AS. GRP78 induction in cancer: therapeutic and prognostic implications. *Cancer Res* 2007; **67**: 3496–3499.
21. Schwarze S, Rangnekar VM. Targeting plasma membrane GRP78 for cancer growth inhibition. *Cancer Biol Ther* 2010; **9**: 153–155.
22. Wu MJ, Jan CI, Tsay YG, Yu YH, Huang CY, Lin SC *et al.* Elimination of head and neck cancer initiating cells through targeting glucose regulated protein78 signaling. *Mol Cancer* 2010; **9**: 283.
23. Martin S, Hill DS, Paton JC, Paton AW, Birch-Machin MA, Lovat PE *et al.* Targeting GRP78 to enhance melanoma cell death. *Pigment Cell Melanoma Res* 2010; **23**: 675–682.
24. Dickson NR JS, Burris HA, Ramanathan RK, Weiss GJ, Infante JR, Bendell JC *et al.* A phase I dose-escalation study of NKP-1339 in patients with advanced solid tumors refractory to treatment. *J Clin Oncol* 2011; **29**: abstract 2607.
25. Cholody WM, Hernandez L, Hassner L, Scudiero DA, Djurickovic DB, Michejda CJ. Bisimidazoacridones and related compounds: new antineoplastic agents with high selectivity against colon tumors. *J Med Chem* 1995; **38**: 3043–3052.
26. Cholody WM, Kosakowska-Cholody T, Hollingshead MG, Hariprakasha HK, Michejda CJ. A new synthetic agent with potent but selective cytotoxic activity against cancer. *J Med Chem* 2005; **48**: 4474–4481.
27. Hariprakasha HK, Kosakowska-Cholody T, Meyer C, Cholody WM, Stinson SF, Tarasova NI *et al.* Optimization of naphthalimide-imidazoacridone with potent antitumor activity leading to clinical candidate (HKH40A, RTA 502). *J Med Chem* 2007; **50**: 5557–5560.
28. Kosakowska-Cholody T, Cholody WM, Monks A, Woynarowska BA, Michejda CJ. WMC-79, a potent agent against colon cancers, induces apoptosis through a p53-dependent pathway. *Mol Cancer Ther* 2005; **4**: 1617–1627.
29. Kosakowska-Cholody T, Cholody WM, Hariprakasha HK, Monks A, Kar S, Wang M *et al.* Growth inhibition of hepatocellular carcinoma cells in vitro and in vivo by the 8-methoxy analog of WMC79. *Cancer Chemother Pharmacol* 2009; **63**: 769–778.
30. Hernandez L, Cholody WM, Hudson EA, Resau JH, Pauly G, Michejda CJ. Mechanism of action of bisimidazoacridones, new drugs with potent, selective activity against colon cancer. *Cancer Res* 1995; **55**: 2338–2345.
31. Wang Z, Wang M, Kar S, Carr BI. Involvement of ATM-mediated Chk1/2 and JNK kinase signaling activation in HKH40A-induced cell growth inhibition. *J Cell Physiol* 2009; **221**: 213–220.
32. Ron D, Walter P. Signal integration in the endoplasmic reticulum unfolded protein response. *Nat Rev Mol Cell Biol* 2007; **8**: 519–529.
33. Hendershot LM, Kearney JF. A role for human heavy chain binding protein in the developmental regulation of immunoglobin transport. *Mol Immunol* 1988; **25**: 585–595.
34. Gulow K, Bienert D, Haas IG. BiP is feed-back regulated by control of protein translation efficiency. *J Cell Sci* 2002; **115**(Pt 11): 2443–2452.
35. Tarasov SG, Casas-Finet JR, Cholody WM, Kosakowska-Cholody T, Gryczynski ZK, Michejda CJ. Bisimidazoacridones: 2. Steady-state and time-resolved fluorescence studies of their diverse interactions with DNA. *Photochem Photobiol* 2003; **78**: 313–322.
36. Seidel SA, Dijkman PM, Lea WA, van den Bogaart G, Jerabek-Willemsen M, Lazic A *et al.* Microscale thermophoresis quantifies biomolecular interactions under previously challenging conditions. *Methods* 2013; **59**: 301–315.
37. Wienken CJ, Baaske P, Rothbauer U, Braun D, Duhr S. Protein-binding assays in biological liquids using microscale thermophoresis. *Nat Commun* 2010; **1**: 100.
38. Jerabek-Willemsen M, Wienken CJ, Braun D, Baaske P, Duhr S. Molecular interaction studies using microscale thermophoresis. *Assay Drug Dev Technol* 2011; **9**: 342–353.
39. Jamora C, Dennert G, Lee AS. Inhibition of tumor progression by suppression of stress protein GRP78/BiP induction in fibrosarcoma B/C10ME. *Proc Natl Acad Sci USA* 1996; **93**: 7690–7694.
40. Tardito S, Isella C, Medico E, Marchio L, Bevilacqua E, Hatzoglou M *et al.* The thioxotriazole copper(II) complex A0 induces endoplasmic reticulum stress and paraptotic death in human cancer cells. *J Biol Chem* 2009; **284**: 24306–24319.
41. Venkatachalam PSaMA. Apoptosis and Cell Death. In: Allen PTCaTC (ed) *Basic concepts of Molecular Pathology*. Springer Science + Business Media, LLC, 2009, pp 29–40.
42. Broker LE, Kruyt FA, Giaccone G. Cell death independent of caspases: a review. *Clin Cancer Res* 2005; **11**: 3155–3162.
43. Sperandio S, Poksay K, de Belle I, Lafuente MJ, Liu B, Nasir J *et al.* Paraptosis: mediation by MAP kinases and inhibition by AIP-1/Alix. *Cell Death Differ* 2004; **11**: 1066–1075.
44. Li Z. Glucose regulated protein 78: a critical link between tumor microenvironment and cancer hallmarks. *Biochim Biophys Acta* 2012; **1826**: 13–22.
45. Cnop M, Ladriere L, Hekerman P, Ortis F, Cardozo AK, Dogusan Z *et al.* Selective inhibition of eukaryotic translation initiation factor 2 alpha dephosphorylation potentiates fatty acid-induced endoplasmic reticulum stress and causes pancreatic beta-cell dysfunction and apoptosis. *J Biol Chem* 2007; **282**: 3989–3997.
46. Lievremont JP, Rizzuto R, Hendershot L, Meldolesi J. BiP, a major chaperone protein of the endoplasmic reticulum lumen, plays a direct and important role in the storage of the rapidly exchanging pool of Ca2 +. *J Biol Chem* 1997; **272**: 30873–30879.
47. Hammadi M, Oulidi A, Gackiere F, Katsogiannou M, Slomianny C, Roudbaraki M *et al.* Modulation of ER stress and apoptosis by endoplasmic reticulum calcium leak via translocon during unfolded protein response: involvement of GRP78. *FASEB J* 2013; **27**: 1600–1609.
48. Martin S, Lamb HK, Brady C, Lefkove B, Bonner MY, Thompson P *et al.* Inducing apoptosis of cancer cells using small-molecule plant compounds that bind to GRP78. *Br J Cancer* 2013; **109**: 433–443.
49. Kimmel AR, Berger SL. Preparation of cDNA and the generation of cDNA libraries: overview. *Methods Enzymol* 1987; **152**: 307–316.

Cell Death and Disease **is an open-access journal published by** ***Nature Publishing Group*****. This work is licensed under a Creative Commons Attribution-NonCommercial-NoDerivs 3.0 Unported License. The images or other third party material in this article are included in the article's Creative Commons license, unless indicated otherwise in the credit line; if the material is not included under the Creative Commons license, users will need to obtain permission from the license holder to reproduce the material. To view a copy of this license, visit http://creativecommons.org/licenses/by-nc-nd/3.0/**

Supplementary Information accompanies this paper on Cell Death and Disease website (http://www.nature.com/cddis)